Crystal-structure refinements of *1M* plutonic biotites

MARIA FRANCA BRIGATTI

Istituto di Chimica, Università della Basilicata, Potenza, Italy

PAOLO DAVOLI

Istituto di Mineralogia e Petrologia, Università di Modena, Italy

ABSTRACT

Crystal-structure refinements were performed on five plutonic *1M* biotite crystals from the three main lithologic complexes (granitic, syenitic, and monzonitic) and from a rock transitional between the granitic and monzonitic complexes of the same plutonic body in the Valle del Cervo (Vercelli, northwestern Italy). All refinements were carried out in the space group $C2/m$ ($R = 0.02$–0.03 for four samples; $R = 0.06$ for one sample).

Although the Valle del Cervo biotite samples show similar chemical composition and crystal-chemical features, structural details as deduced from ΔF maps suggest different orientations of OH^- groups in samples from different plutonic complexes.

Structural details of the biotites show that (1) octahedral-layer distortion in more Mg-rich biotites is greater (and analogous in M1 and M2 sites) than that in more Fe-rich biotites, where the "average" distortion of the octahedral layer decreases with increasing Fe content and the M1 site is more distorted and larger than the M2 site; (2) the reduction in ⟨M-O⟩ distance in the two octahedra causes a more marked reduction in the size of the M2 sites as compared with the M1 site; (3) octahedral geometrical parameters are affected both by their chemical composition and by the constraints of close packing within the layer; and (4) tetrahedral-ring distortion is not affected by the octahedral composition, whereas it is linked to the geometry of the ditrigonal cavity occupied by the interlayer cation.

INTRODUCTION

The basic mica structure was outlined by Pauling (1930) and refined many times. Although much attention has been given to the crystal chemistry of dioctahedral micas, the various trioctahedral Fe-Mg micas have received less attention (Bergerhoff et al., 1986). Of the latter, phlogopite has been studied most extensively, whereas annite, as well as micas along the phlogopite-annite join (biotites), are less understood. The recent literature contains no studies of crystal refinements of biotite from plutonic rocks; only biotites from volcanic and metamorphic rocks have been reported (Takeda and Ross, 1975; Bohlen et al., 1980), and only one *1M* biotite has been described (Takeda and Ross, 1975; Ohta et al., 1982). A detailed crystal-chemical study of five *1M* biotite samples from three lithologic complexes (granitic, syenitic, and monzonitic) and from a rock transitional between the granitic and monzonitic complexes in the same plutonic body is reported in order to assess to what extent petrologic conditions affect the crystal-chemical features of biotite.

EXPERIMENTAL

Samples

The five *1M* biotite crystals used for structure refinements were chosen from the three main lithologic complexes of the Valle del Cervo pluton (Vercelli, north-

western Italy): granitic (sample M13), syenitic (sample M32), monzonitic (samples M14 and M73), and a rock transitional between the granitic and monzonitic complexes (sample M62). The bulk chemical compositions of the rocks cover a wide range (Table 1).

X-ray single-crystal diffractometry

Single-crystal diffraction analysis is more difficult for micas than for many other rock-forming silicates because the mica crystals are often deformed and are very thin and platy. These features cause the diffraction peaks to be broad and to require relatively significant corrections for absorption. Special attention was therefore paid to experimental procedures, sample selection, and collection parameters in order to ensure reliable data and refinement results.

About 70 biotite crystals were examined preliminarily by Weissenberg or precession photography and by single-crystal diffractometry to select samples with well-defined periodicity along c^*. In all five rock samples *1M*, *2M₁*, and disordered stacking sequences were found; in granitic and syenitic rock samples, the *3T* polytype was also found.

The cell parameters and the diffraction intensities were measured for each of the five samples. Each was mounted along the **b** axis. Intensity data were measured with an ENRAF-NONIUS CAD4 diffractometer using $MoK\alpha$ radiation and a flat graphite crystal monochromator. During inten-

TABLE 1. Samples of Valle del Cervo plutonic complex: Bulk-rock chemical composition

Sample	Rock type	SiO₂	Al₂O₃	TiO₂	FeO	MgO	MnO	CaO	Na₂O	K₂O	P₂O₅
M14	Monzonite	59.07	14.95	0.81	5.70	3.53	0.11	5.79	3.26	6.38	0.81
M32	Syenite	63.40	15.87	0.48	4.19	2.15	0.09	4.05	3.76	5.57	0.44
M13	Granite	67.78	15.86	0.38	2.77	1.32	0.07	3.06	3.80	4.72	0.24
M73	Monzonite	55.14	15.63	0.79	6.35	4.21	0.13	6.24	3.72	5.65	0.92
M62	Transitional*	64.45	14.61	0.09	5.68	2.50	0.12	4.57	3.79	4.19	nd

* Rock transitional between granitic and monzonitic complexes.

sity collection the maximum variation of selected standard reflections did not exceed 2.5%. The equivalent monoclinic pairs *hkl* and *hkl* were measured from $\theta = 2°$ to $\theta = 30°$ (*l* starting from *l* = 0).

The $(\Delta\omega, \Delta\theta)$ plots (Einstein, 1974) showed a high degree of broadening along $\Delta\omega$ direction, and therefore the omega scan mode was chosen to ensure complete measurement of each peak intensity; the choice of a horizontal detector aperture as small as possible (between 0.3° and 1.0°, as the angle is viewed from the crystal) ensured a high peak to background resolution (Davoli, 1989). Scan widths were 5°–6° in ω for samples M14, M32, M73, and M62 and 10° in ω for sample M13.

The intensities were corrected for Lorentz-polarization and absorption effects following the semiempirical method of North et al. (1968); intensity data of symmetrically equivalent reflections were averaged. The resulting discrepancy factor R_{sym} was calculated as reported in Table 3.

Chemical analyses

Electron-probe microanalyses (EPMA) were performed with an ARL-SEMQ instrument using wavelength-dispersive techniques. Operating conditions were a 15-*kV* accelerating voltage, a 15-nA sample current, and a defocused electron beam (spot size of about 3 μm). Spectrometer data were reduced using the method of Ziebold and Ogilvie (1964) with correction factors of Albee and Ray (1970). Six analyses from different points on the same crystal showed high chemical homogeneity, and therefore these were averaged.

Atomic absorption analysis revealed that the amount of Li never exceeded 0.05 wt%. OH was determined by means of thermogravimetric analysis (TG and DTG) on crystals from the same rock. A Du Pont 990 thermal analyzer was used on about 10 mg of powder heated at the rate of 10 °C/min in Ar gas (flow rate, 30 ml/min) to prevent Fe oxidation. Fe^{3+} was determined by a semimicrovolumetric method (Meyrowitz, 1963). Structural formulae were calculated on the basis of O + OH + Cl = 24 (Table 2).

TABLE 2. Chemical compositon of biotites studied

	M14	M32	M13*	M73	M62
SiO₂	36.50	37.44	36.74	36.05	36.25
Al₂O₃	13.20	13.77	13.21	14.20	13.90
TiO₂	4.03	2.72	3.95	4.38	3.39
Fe₂O₃	8.39	8.13	5.80	6.24	6.80
FeO	12.34	11.41	14.00	13.53	14.81
MgO	12.62	13.49	11.70	12.23	11.80
MnO	0.19	0.43	0.50	0.23	0.49
Li₂O	0.03	0.04	0.05	0.02	0.03
Na₂O	0.17	0.08	0.08	0.14	0.10
K₂O	9.24	9.67	10.02	9.36	9.57
CaO	0.00	0.06	0.02	0.00	0.00
H₂O	3.00	3.47	2.80	3.21	2.80
Cl	0.30	0.14	0.30	0.41	0.06
Si	5.561	5.595	5.692	5.484	5.581
Al	2.370	2.405	2.308	2.516	2.419
Fe³⁺	0.069	—	—	—	—
Sum	8.000	8.000	8.000	8.000	8.000
Al	—	0.021	0.104	0.030	0.104
Fe³⁺	0.893	0.914	0.676	0.714	0.788
Fe²⁺	1.572	1.426	1.814	1.721	1.907
Mg	2.865	3.005	2.701	2.773	2.707
Mn	0.025	0.054	0.066	0.030	0.064
Ti	0.462	0.306	0.460	0.501	0.392
Li	0.018	0.024	0.031	0.012	0.019
Sum	5.835	5.750	5.852	5.781	5.981
Ca	—	0.010	0.003	—	—
Na	0.050	0.023	0.024	0.041	0.030
K	1.796	1.844	1.980	1.816	1.880
Sum	1.846	1.877	2.007	1.857	1.910
OH	3.049	3.459	2.893	3.257	2.875
Cl	0.077	0.035	0.032	0.106	0.016
O	20.874	20.506	21.075	20.637	21.109
Sum	24.000	24.000	24.000	24.000	24.000

* H₂O⁻ = 1.00.

Crystal-structure refinement

The crystal-structure refinements of *1M* biotites were carried out without chemical constraints, using a version of the least-squares program ORFLS (Busing et al., 1962), rewritten at the Centro di Studio per la Cristallografia Strutturale of Pavia and revised locally. The program allows the assignment of two scattering curves f_1 and f_2 to every site affected by isomorphous replacement and refinement of the site occupancy X(f) with the constraint that X(f_1) + X(f_2) = 1. The choice of the scattering factors was Fe^{2+} versus Mg^{2+} for M1 and M2, a composite of 75% Si and 25% Al versus 75% Si^{4+} and 25% Al^{3+} in site T, and O versus O^{2-} (Tokonami, 1965) for anion sites.

Fully ionized atomic scattering factors were used for sites M1 and M2 in order to obtain better final R factors and estimated standard deviations of the refined parameters. It was assumed, on the basis of chemical analyses and bond lengths, that T is occupied by 0.75 Si and 0.25 Al, and, owing to the small difference between Al and Si scattering curves, no least-squares refinement of Al versus Si was carried out.

TABLE 3. Crystallographic data and parameters of the biotites studied

	M14	M32	M13	M73	M62
Dimensions (mm)	$0.28 \times 0.25 \times 0.06$	$0.12 \times 0.08 \times 0.03$	$0.17 \times 0.14 \times 0.04$	$0.15 \times 0.10 \times 0.02$	$0.24 \times 0.15 \times 0.02$
N_{all}	562	276	476	460	342
N_{obs}	477	254	387	422	305
$R_{sym} (\times 100)^*$	3.3	3.3	4.7	2.4	4.6
$R_{all} (\times 100)$	3.9	2.6	8.3	2.5	4.8
$R_{obs} (\times 100)$	3.3	2.4	6.2	2.1	3.5
a (Å)	5.343(3)	5.346(2)	5.355(1)	5.345(1)	5.337(1)
b (Å)	9.258(1)	9.252(2)	9.251(4)	9.258(2)	9.242(2)
c (Å)	10.227(2)	10.238(4)	10.246(4)	10.222(2)	10.211(2)
β (°)	100.26(2)	100.02(3)	100.15(3)	100.23(2)	100.15(2)
V (Å³)	497.8	498.7	499.6	497.8	495.8

Note: Entries in column 1 are sample size, number of total and observed reflections, agreement factors and lattice parameters. Esd's on the last significant digit are in parentheses.
* $R_{sym} = (\Sigma_{hkl}\Sigma_{i=1}^{N}|I_{(hkl)_i} - I_{hkl}|)/\Sigma_{hkl}\Sigma_{i=1}^{N}I_{hkl}$.

All the refinements were carried out in space group $C2/m$ in the same coordinate setting as reported by Takeda and Ross (1975). Only reflections with $I > 5\sigma(I)$ were used in order to reduce the standard deviations of the refined parameters without loss of statistically significant F_{obs} in least-square cycles. (For applications of these refinement procedures to other rock-forming minerals, see Ungaretti, 1980; Ungaretti et al., 1983; Davoli, 1987.)

During refinement cycles, occupancy factors and thermal parameters were varied separately; attempts to vary all parameters simultaneously gave a higher R factor and higher estimated standard deviations and correlation coefficients.

An attempt was made to refine sample M13 in space groups $C2$ and Cm. In order to avoid false R minima or high correlations between couples of pseudo-related atoms in the lower-symmetry space groups, atoms related by pseudo-symmetry elements were shifted from their positions and refined in separate least-squares cycles. No enhanced results (Hamilton, 1965) were found.

Unit-cell parameters (obtained by least-squares refinement of 25 automatically centered reflections in the range $15° \leq \theta \leq 30°$) and some refinement data are in Table 3. Crystallographic coordinates and equivalent isotropic and anisotropic temperature factors are in Table 4. A list of observed and calculated structure factors for all samples is in Table 5.[1] Relevant bond distances, angles, and polyhedral distortion parameters are in Table 6. Mean atomic numbers of cation sites, as estimated by structure refinement and EPMA, are also reported and compared in Table 7.

SOME STRUCTURAL FEATURES BY ΔF FOURIER MAP ANALYSIS

At the end of the anisotropic refinement a difference (ΔF) Fourier synthesis was computed. The standard deviation for the estimation of electron density (as calcu-

lated by Lipson and Cochran, 1953) for the samples under inspection ranges between 0.04 and 0.08 e/Å³. A careful examination of the final ΔF maps shows significant peaks that can result from two different causes: positions of H atoms and disorder or twinning phenomena.

Samples M73, M14, M32

According to Bailey (1984), the position of H is expected to be 0.90–0.95 Å from the O4 location. The OH vector is perpendicular to the octahedral sheet and is directed toward the ditrigonal cavity in trioctahedral micas, whereas this vector is expected to lie in the (001) plane toward the vacant M1 octahedron in dioctahedral micas; e.g., in a neutron refinement of a phlogopite, Joswig (1972) located the H proton at (0.098, 0.5, 0.3007) at 1.003 Å from O4, with the OH vector normal to the (001) plane.

In both samples M73 and M14 (monzonitic complex) the most relevant ΔF peak (1.0 e/Å³ in both samples) suggests a plausible H location with atomic coordinates (0.09, 0.5, 0.315) at 0.81 Å from O4, with the OH vector almost normal to plane (001). In sample M32 (syenitic complex) the most relevant ΔF peak (0.94 e/Å³) suggests a possible H location with atomic coordinates (0.010, 0.5, 0.315) at 0.97 Å from O4, with the OH vector slightly tilted to (001) plane.

Sample M13

Sample M13 shows the worst refinement results: at the end of anisotropic refinement the R value was 0.06 and the esd's are considerably higher than those of other samples. ΔF map shows unusual features, with a peak (1.2 e/Å³) in a position corresponding to a shift of $b/3$ for atom T along the b axis, and a smaller peak (0.9 e/Å³) in a position corresponding to a K-site shift of $\pm b/3$.

A sample from the same rock type (sample M105, whose refinement is not reported since the R value cannot be reduced below 0.11 in the standard $1M$ model) exhibits similar behavior with enhanced features: the ΔF map shows peaks corresponding to a complete superimposition of a 2:1 layer structure shifted by $\pm b/3$ to the basic mica structure. The following five peaks are found: $T + b/3$, $K + b/3$ (and $K - b/3$ due to the m plane), O2

---

[1] A copy of Table 5 may be ordered as Document AM-90-427 from the Business Office, Mineralogical Society of America, 1625 I Street, N.W., Suite 414, Washington, D.C. 20006, U.S.A. Please remit $5.00 in advance for the microfiche.

TABLE 4. Crystallographic coordinates and equivalent isotropic ($Å^2$) and anisotropic ($Å^2 \times 10^4$) temperature factors for *1M* biotites studied

Atom	x/a	y/b	z/c	B_{eq}	β_{11}*	β_{22}*	β_{33}*	β_{12}*	β_{13}*	β_{23}*
Sample M14										
O1	0.0268(8)	0.0	0.1690(4)	2.3(1)	286(18)	41(4)	57(5)	0	21(8)	0
O2	0.3192(5)	0.2357(3)	0.1682(3)	2.11(7)	198(10)	70(4)	45(3)	−34(5)	26(4)	−7(3)
O3	0.1312(5)	0.1678(3)	0.3912(3)	1.60(6)	150(8)	46(3)	40(3)	−4(4)	25(4)	−2(3)
O4	0.1286(7)	0.5	0.3957(4)	1.72(9)	156(13)	40(4)	53(4)	0	29(7)	0
M2	0.0	0.3348(1)	0.5	1.47(3)	133(4)	40(1)	40(1)	0	23(2)	0
M1	0.0	0.0	0.5	1.36(4)	133(5)	29(2)	43(2)	0	31(3)	0
K	0.0	0.5	0.0	3.39(6)	306(9)	95(3)	89(3)	0	39(4)	0
T	0.0749(2)	0.1668(1)	0.2258(1)	1.33(2)	131(3)	31(1)	39(1)	−1(2)	26(2)	0(1)
Sample M32										
O1	0.0236(12)	0.0	0.1681(6)	1.6(2)	173(28)	48(8)	29(6)	0	−3(10)	0
O2	0.3221(8)	0.2339(5)	0.1695(4)	1.7(1)	153(17)	61(7)	32(4)	−11(9)	13(7)	0(5)
O3	0.1308(7)	0.1673(6)	0.3910(4)	1.2(1)	128(18)	33(6)	27(5)	12(14)	4(8)	−7(6)
O4	0.1293(13)	0.5	0.3960(7)	1.4(2)	130(32)	40(11)	35(9)	0	29(14)	0
M2	0.0	0.3340(3)	0.5	0.89(6)	56(8)	27(3)	28(2)	0	4(4)	0
M1	0.0	0.0	0.5	0.91(9)	104(14)	22(4)	22(4)	0	16(6)	0
K	0.0	0.5	0.0	2.7(1)	222(14)	84(5)	68(4)	0	20(6)	0
T	0.0752(3)	0.1674(2)	0.2262(1)	0.85(4)	74(6)	22(2)	23(2)	7(7)	5(3)	2(3)
Sample M13										
O1	0.0241(18)	0.0	0.1694(9)	2.6(2)	242(37)	71(12)	65(10)	0	35(15)	0
O2	0.3203(11)	0.2355(7)	0.1668(6)	2.5(2)	213(23)	81(9)	64(6)	−20(12)	45(10)	−4(7)
O3	0.1330(9)	0.1676(6)	0.3916(5)	1.4(1)	105(17)	31(5)	50(6)	−5(10)	17(8)	1(6)
O4	0.1304(14)	0.5	0.3949(7)	1.4(2)	131(29)	48(9)	28(8)	0	18(12)	0
M2	0.0	0.3342(3)	0.5	1.62(5)	115(7)	54(3)	44(2)	0	23(3)	0
M1	0.0	0.0	0.5	1.56(8)	136(11)	43(4)	45(3)	0	30(5)	0
K	0.0	0.5	0.0	3.6(1)	306(20)	106(7)	100(6)	0	54(9)	0
T	0.0752(4)	0.1666(2)	0.2256(2)	1.26(5)	95(7)	35(2)	41(2)	−7(4)	24(3)	−3(3)
Sample M73										
O1	0.0267(6)	0.0	0.1687(3)	1.71(8)	224(13)	35(3)	33(3)	0	1(5)	0
O2	0.3195(4)	0.2361(3)	0.1681(2)	1.66(5)	141(7)	60(3)	34(2)	−28(4)	17(3)	−7(2)
O3	0.1316(3)	0.1677(2)	0.3909(2)	1.03(4)	86(6)	30(2)	27(2)	3(4)	9(3)	−3(2)
O4	0.1291(5)	0.5	0.3947(3)	1.16(8)	76(10)	22(4)	47(4)	0	16(5)	0
M2	0.0	0.3347(1)	0.5	1.00(2)	61(3)	32(1)	30(1)	0	7(1)	0
M1	0.0	0.0	0.5	0.93(3)	76(4)	20(1)	33(1)	0	16(2)	0
K	0.0	0.5	0.0	2.95(5)	255(7)	80(2)	80(2)	0	24(3)	0
T	0.0748(1)	0.1669(1)	0.2257(1)	0.76(2)	58(2)	18(1)	25(1)	−1(2)	7(1)	−1(1)
Sample M62										
O1	0.0239(14)	0.0	0.1698(9)	2.0(2)	220(31)	32(8)	57(10)	0	16(14)	0
O2	0.3207(9)	0.2340(6)	0.1681(6)	2.0(1)	115(16)	72(7)	61(6)	−26(9)	31(8)	−5(6)
O3	0.1303(7)	0.1676(6)	0.3909(5)	1.3(1)	64(15)	20(5)	62(7)	1(11)	24(9)	1(7)
O4	0.1305(12)	0.5	0.3952(7)	1.0(2)	96(27)	38(10)	16(9)	0	1(13)	0
M2	0.0	0.3350(3)	0.5	1.29(5)	80(6)	40(2)	41(3)	0	17(4)	0
M1	0.0	0.0	0.5	1.20(8)	75(10)	36(4)	40(4)	0	20(5)	0
K	0.0	0.5	0.0	3.0(1)	245(15)	82(5)	89(6)	0	26(8)	0
T	0.0746(3)	0.1666(2)	0.2255(2)	0.91(4)	43(5)	20(2)	40(2)	1(5)	15(3)	3(3)

Note: Esd's on the last significant digit are in parentheses.
* $\exp[-(h^2\beta_{11} + \cdots + 2hk\beta_{12} + \cdots)]$.

+ **b**/3, O2 − **b**/3, and O1 + **b**/3 (plus O1 − **b**/3 due to the *m* plane).

Smith and Yoder (1956) emphasized that a [310] or [3$\bar{1}$0] twin axis causes two structures with a reciprocal ±**b**/3 shift. Bell and Wilson (1977, 1981), on the basis of TEM observations, found growth defects in metamorphic biotites with stacking modes, among which ±**b**/3 is present, corresponding to microtwins of a few unit cells. On the basis of energetic considerations, they suggested that the shift should occur in the octahedral layer. On the other hand, Gregorkiewitz and Rausell-Colom (1987) report a new synthetic 2:1 layer silicate with a suggested ±**b**/3 shift in the interlayer region between the bases of two adjacent tetrahedral layers.

In samples M13 and M105 no macroscopic twin was observed, but preliminary TEM observations (S. Bigi, personal communication) of samples from the same granitic complex as M105 show a predominate *1M* structure with small domains containing microtwins on one of the following axes: [310] and [3$\bar{1}$0] or [110] and [1$\bar{1}$0]. In samples M13 and M105 the presence of peaks in the ΔF map that are related by ±**b**/3 can therefore be explained as coherently diffracting small domains with a ±**b**/3 shift with respect to the dominant 1M matrix (Rule et al., 1987). According to this hypothesis, and referring to the "complete" set of ΔF maxima of sample M105, it should be noted that, owing to the (010) symmetry plane, no other ΔF maximum corresponding to an atomic ±**b**/3 shift is to be expected. The presence of these microtwins does not invalidate the substantial correctness of the crys-

TABLE 6. Selected data from structure refinements of *1M* biotites

	M14	M32	M13	M73	M62
T-O1	1.654(2)	1.665(3)	1.651(4)	1.655(1)	1.648(4)
T-O2	1.653(3)	1.650(5)	1.664(6)	1.656(2)	1.652(5)
T-O2'	1.656(3)	1.652(5)	1.661(6)	1.652(2)	1.657(5)
T-O3	1.664(3)	1.662(4)	1.674(6)	1.662(2)	1.662(5)
⟨T-O⟩	1.657	1.657	1.663	1.656	1.654
TQE	1.0003	1.0003	1.0006	1.0003	1.0002
α (°)	5.66	6.37	5.72	5.50	6.31
M1-O3 (×4)	2.103(3)	2.098(5)	2.104(5)	2.105(2)	2.097(5)
M1-O4 (×2)	2.079(4)	2.080(7)	2.080(7)	2.081(3)	2.071(7)
⟨M1-O⟩	2.095	2.092	2.096	2.097	2.089
OQE	1.0114	1.0107	1.0110	1.0106	1.0103
ψ (°)	58.98	58.86	58.90	58.85	58.79
e_u/e_s	1.1073	1.1041	1.1055	1.1036	1.1024
M2-O3 (×2)	2.097(3)	2.094(5)	2.096(5)	2.100(2)	2.096(6)
M2-O3' (×2)	2.083(3)	2.092(4)	2.080(5)	2.084(2)	2.088(4)
M2-O4 (×2)	2.051(3)	2.056(5)	2.065(5)	2.059(2)	2.054(5)
⟨M2-O⟩	2.077	2.080	2.081	2.081	2.079
OQE	1.0099	1.0098	1.0097	1.0093	1.0096
ψ (°)	58.69	58.66	58.66	58.58	58.62
e_u/e_s	1.0996	1.0992	1.0988	1.0969	1.0982
K-O1 (×2)	3.029(5)	3.020(6)	3.029(9)	3.029(3)	3.019(8)
K-O1' (×2)	3.307(5)	3.313(7)	3.327(9)	3.305(3)	3.319(8)
K-O2 (×4)	3.288(3)	3.317(4)	3.289(7)	3.286(2)	3.299(6)
K-O2' (×4)	3.041(3)	3.029(5)	3.028(6)	3.041(2)	3.020(6)
⟨K-O⟩inner	3.037	3.026	3.029	3.037	3.020
⟨K-O⟩outer	3.294	3.316	3.308	3.292	3.306
Δ(K-O)*	0.257	0.290	0.273	0.255	0.286

Note: Entries in column 1 are bond distances (Å); TQE, OQE (after Robinson et al., 1971); octahedral flattening angles ψ and tetrahedral rotation angle α (after Hazen and Burnham, 1973); e_u/e_s (after Toraya, 1981). Esd's on the last significant digit are in parentheses.
* ⟨K-O$_{outer}$⟩ − ⟨K-O$_{inner}$⟩.

tal chemical model refined for sample M13. (See also Davoli, 1989, for an operative discussion of accuracy and precision in structure refinement results of natural samples.)

Sample M62

Sample M62 was refined to an *R* value of 0.03. The analysis of its ΔF map shows two most relevant peaks (both 1.0 e/Å³), one at (0.09, 0.50, 0.315) at 0.81 Å from O4, and the other in a position corresponding to a shift of atom T by **b**/3. The former peak corresponds to the possible location of the H atoms similar to that inferred in samples M73 and M14 (monzonitic complex). The latter corresponds to the T site shift of ±**b**/3 found in sample M13 (granitic complex). Sample M62 represents a transition between monzonitic and granitic complexes.

DISCUSSION

Valle del Cervo *1M* biotites from different rock types show similar chemical compositions (Table 2) and crystal-chemical features (Tables 3, 6, 7). These features are similar to those observed by Bohlen et al. (1980) for a *2M₁* polytype and extend analogous conclusions to the plutonic environment and to the *1M* polytype. However, some differences in structural details as deduced from ΔF maps (e.g., different positions of H when biotites from monzonitic and syenitic complexes were compared, presence of microtwins in samples from granitic rocks) may result from differences in rock chemistry.

The number of electrons associated with each cation site, as calculated by EPMA, corresponds well with that calculated by X-ray refinement. The agreement is not as good for sample M13; the above discussion on microtwins related to ±**b**/3 shifts could suggest the presence of microdomains with a slightly different composition in the sample.

The discussion of thermal factors is sometimes neglected in crystal chemical works because many authors think they only incorporate the errors of data collection and structure refinement. Even if this statement is largely true, some useful auxiliary information can, nevertheless, be deduced from their analysis. Reference should be made,

TABLE 7. Mean atomic number of octahedral and interlayer sites as determined by structure refinement and microprobe analysis for *1M* biotites studied

	M14	M32	M13	M73	M62
M1*	18.61(8)	17.9(1)	20.4(1)	18.96(7)	20.4(1)
M2*	17.8(1)	17.1(2)	19.8(2)	18.2(1)	19.6(2)
K*	18.66(6)	18.8(1)	18.5(1)	18.92(5)	19.4(1)
(M1 + M2)*‡	54.2	52.1	60.0	55.4	59.6
(M1 + M2)†§	54.7	52.7	55.2	54.2	57.1
K†	17.3	17.7	19.0	17.4	18.0

Note: Esd's on the last significant digit are in parentheses.
* X-ray refinement.
† Electron-microprobe analysis.
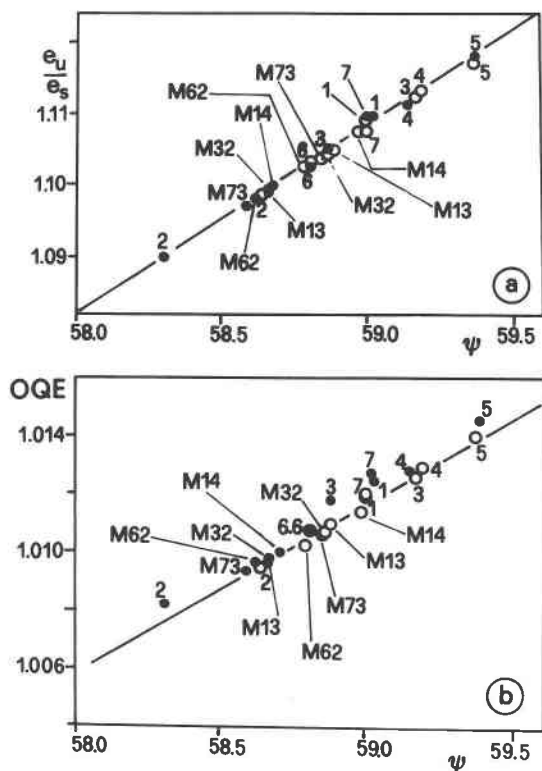‡ (2 × M2) + M1.
§ Sum of octahedral-cation electrons.

Fig. 1. (a) e_u/e_s vs. ψ (in degrees) and (b) OQE vs. ψ (in degrees) in the phlogopite-annite join for M1 (open circles) and M2 (solid circles) octahedra. Samples M14, M32, M13, M73, and M62 from this study; 1, phlogopite (Hazen and Burnham, 1973); 2, annite (Hazen and Burnham, 1973); 3, biotite (Takeda and Ross, 1975); 4, phlogopite (Joswig, 1972); 5, fluorophlogopite (Takeda and Morosin, 1975); 6, phlogopite (Hazen et al., 1981); and 7, fluorophlogopite (McCauley et al., 1973).

Fig. 2. OQE vs. mean $\langle M\text{-}O\rangle$ (in Å) distance in the phlogopite-annite join for M1 and M2 octahedra. Symbols and samples as in Fig. 1. Dashed lines: M1; solid lines: M2.

however, only to their relative and not their absolute values.

In all the samples, thermal factors are quite high, probably due to layer disorder, but they do not show distinct anisotropies. They are also remarkably consistent with the crystal-chemical nature of the respective sites (Vainshtein, 1981, p. 233; Stout and Jensen, 1968, p. 206): the tetrahedral atoms (T) show the lowest B_{eq}, K the greatest, and the M1 and M2 atoms have B_{eq} just slightly higher than those of the tetrahedral sites, in accordance with the stronger or weaker bonds affecting each site (Table 4). Of the oxygens, the O1 and O2 basal pair, which coordinate tetrahedral and interlayer atoms, exhibit higher thermal factors than the O3 and O4 pair, which coordinate the tetrahedral and octahedral atoms. This suggests that the atomic position of the former is less well defined than that of the latter (see discussion on ψ and α below).

Octahedral layer

The parameters we used to measure octahedral distortions are (1) ψ (Donnay et al., 1964; formula as in Hazen and Burnham, 1973)—ψ is the octahedral flattening an-
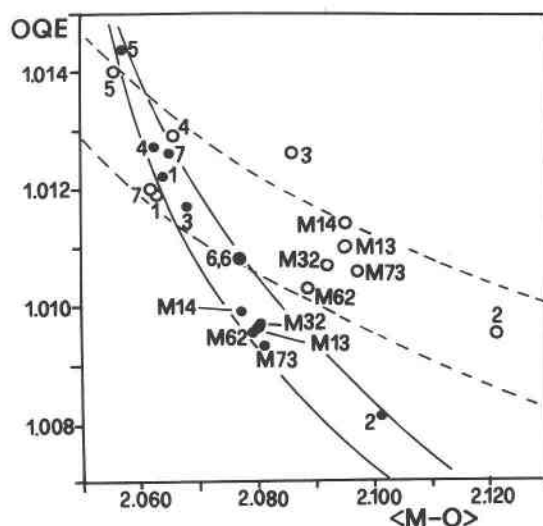
gle; (2) e_u/e_s (Toraya, 1981)—e_u and e_s are the mean lengths of unshared and shared octahedral edges, respectively, and their ratio measures the distortion that each octahedron undergoes by being inserted into layers with shared edges; and (3) OQE (Robinson et al., 1971)—octahedral quadratic elongation, a distortion parameter widely used for chain-silicate minerals (e.g., Rossi et al., 1983; Rossi, 1987; Davoli, 1987).

In order to study the variation of geometric parameters in the phlogopite-annite series, of which the studied samples are intermediate in chemistry, we examined data reported in the literature (Fig. 1). Toraya (1981) showed an excellent correlation between e_u/e_s and ψ for *1M* endmember silicate and germanate micas. This correlation exists also for the intermediate samples examined, as shown in Figure 1a (regression equation: $e_u/e_s = -0.4276 + (2.603 \times 10^{-2})\psi$; $r = 0.999$, in accordance with Toraya, 1981). In Figure 1b, OQE is plotted against ψ and shows a trend similar to that in 1a, although with a slightly lower correlation (regression equation: OQE = 0.660 + (5.96 $\times 10^{-3})\psi$; $r = 0.982$).

Figure 2 shows the OQE distortion trend versus the mean distance $\langle M\text{-}O\rangle$ in M1 and M2, respectively.

Figure 3 plots the graph $\Delta(M\text{-}O) = (\langle M1\text{-}O\rangle - \langle M2\text{-}O\rangle)$ against $\Delta(e_u/e_s) = (e_u/e_s)_{M1} - (e_u/e_s)_{M2}$ (regression equation: $\Delta(e_u/e_s) = 0.42\Delta(M\text{-}O)$; $r = 0.998$).

Figure 1 shows that the octahedral-sheet distortion is similar in both M1 and M2. As the Fe content increases, the average distortion of the layer decreases and the two octahedra become more distinct: M1 is more distorted and larger than M2 (Fig. 2). The number of electrons associated with site M1 is slightly higher than that associated with M2 (Table 7), thereby suggesting a slight pref-
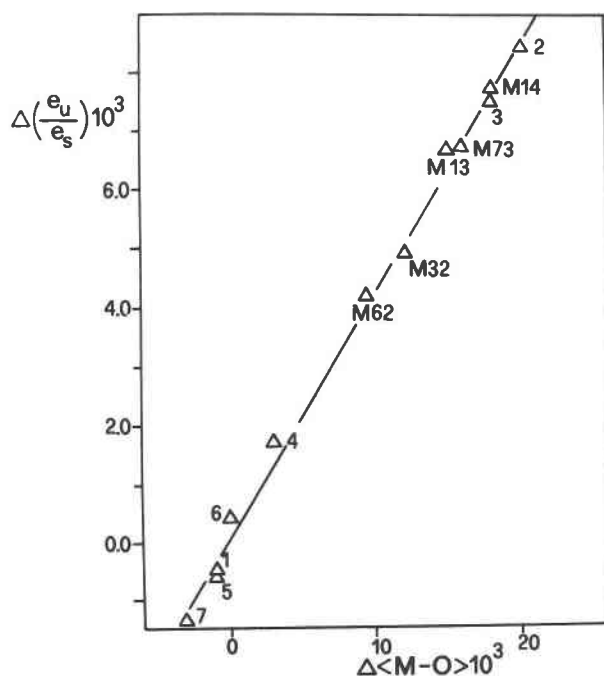
Fig. 3. $\Delta(e_u/e_s) = (e_u/e_s)_{M1} - (e_u/e_s)_{M2}$ vs. $\Delta(M\text{-}O) = (\langle M1\text{-}O\rangle - \langle M2\text{-}O\rangle)$. Samples as in Fig. 1.

Fig. 4. $\langle M\text{-}O\rangle$ (in Å) distance vs. mean $\langle T\text{-}O\rangle$ (in Å) distance for M1 and M2 octahedra. Symbols and samples as in Fig. 1. Vertical lines: phlogopite field; horizontal lines: biotite and annite field.

erence of Fe^{2+} for M1, in accordance with the observation of Bohlen et al. (1980) for a $2M_1$ polytype biotite.

Figure 2 clearly shows the difference in the rate of decrease of the OQE distortion in the two octahedra as a result of an increase in the average M-O distances. This difference between M1 and M2 is also evident in Figure 3, where the effect of a difference in the octahedra distortion $\Delta(e_u/e_s)$ resulting from size differences $\Delta(M\text{-}O)$ is shown. The correlation is high ($r = 0.998$). Phlogopites, biotites, and annites are found in fairly well-defined fields.

Some observations can be made about structural details of the octahedral layer. First, in annite (sample 2) the two octahedra have a similar composition but different topology (size and distortion) (Figs. 1, 2). The converse can be observed in Figures 1 and 3 where it is shown that the biotite samples with small amounts of small, highly charged octahedral cations (Al, Ti^{4+}, Fe^{3+}) behave like those with large amounts (and therefore a different composition) and therefore fall on the same linear trends. Finally, chain silicates with less closely packed octahedral structures exhibit geometrical distortions in contrast with those observed in this study for M1 and M2 in biotites, showing octahedra with distortions that vary inversely with the size of occupying cation (Ghose et al., 1986; Davoli, 1987; Rossi, 1987). These observations suggest that the structural topology in trioctahedral micas is influenced not only by composition but also by the constraints of closest packing within the layer and the confinement of the octahedron between opposite tetrahedral sheets (see also Weiss et al., 1985; Lin and Guggenheim, 1983).
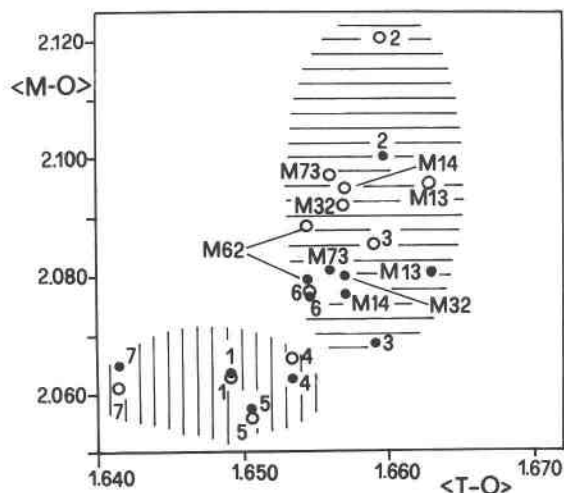
Tetrahedral layer and interlayer

The tetrahedral geometrical parameters we used are (1) α (Newnham and Brindley, 1956; formula as in Hazen and Burnham, 1973)—the tetrahedral rotation angle and (2) TQE (Robinson et al., 1971)—the tetrahedral quadratic elongation, similar to OQE.

The tetrahedra in the biotites analyzed are very regular, as indicated by the tetrahedral distortion parameter (TQE) with values between 1.0003 and 1.0005. These values are similar to those of phlogopites and annites reported elsewhere. The tetrahedral distortion is not affected by the octahedral composition.

Figure 4 gives the mean distance $\langle T\text{-}O\rangle$ versus $\langle M1\text{-}O\rangle$ and $\langle M2\text{-}O\rangle$ and shows two fields for phlogopites and biotites; the former fall into the field $\langle T\text{-}O\rangle$ and $\langle M\text{-}O\rangle$ less than 1.655 Å and 2.067 Å respectively, the latter into a field of higher values. The difference in the mean $\langle T\text{-}O\rangle$ distance reported in Figure 4 does not seem to be due solely to slight differences in the amount of tetrahedral Al (viz. the data reported in Table 2 and the literature quoted in the caption to Fig. 1). Thus, an increase in the $\langle T\text{-}O\rangle$ dimension seems to be linked to an increase in $\langle M\text{-}O\rangle$, although only qualitatively.

Various authors (e.g., Toraya, 1981; Takeda and Morosin, 1975; Hazen and Burnham, 1973) have suggested a close relationship between the tetrahedral ring rotation angle, α, with both the flattening angle, ψ, and the composition of the octahedral sheet. Figure 5, however, shows that a significant correlation between ψ and α does not exist. This is not surprising. First, the greater thermal parameters of basal oxygens O1 and O2 as compared with octahedral oxygens O3 and O4 (see above) suggest that, because of the less close and rigid packing of the tetrahedral layer, O1 and O2 have less well-defined atomic positions than O3 and O4, and the parameter α would
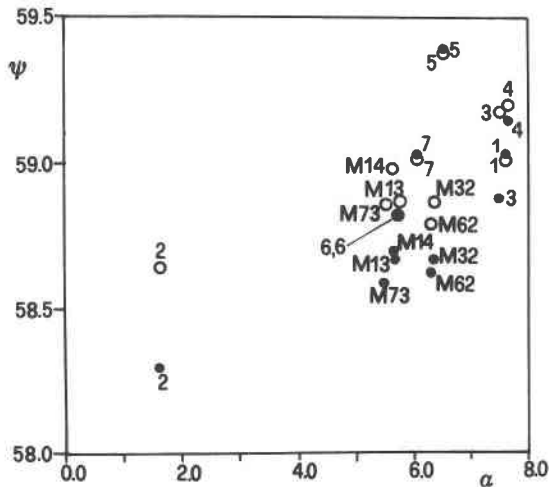
Fig. 5. ψ octahedral flattening angle (in degrees) vs. α tetrahedral rotation angle (in degrees) in the phlogopite-annite join for M1 and M2 octahedra. Symbols and samples as in Fig. 1.

therefore be more affected than the parameter ψ (or e_u/e_s). Secondly, it can be seen that α does not distinguish crystals with different octahedral compositions, such as phlogopites ($\alpha = 5.7–7.7$, samples 1, 4–7) and biotites ($\alpha = 5.5–7.5$, samples 3, M32, M73, M14, M13, M62).

As a consequence, a statistical regression analysis between α and the main octahedral geometric parameters does not show a correlation, and angle α, therefore, appears to be less significant in describing structural modifications linked with the chemistry of the crystal than ψ (or e_u/e_s) (Figs. 1 and 3).

Angle α is, however, linked to the geometry of the ditrigonal cavity occupied by the interlayer cation. Since $\Delta(K-O)$ is the difference between mean distance $K-O_{outer}$ and $K-O_{inner}$, a good positive correlation with α is found (regression equation $\Delta(K-O) = (-4.29 \times 10^{-3}) + (4.62 \times 10^{-2})\alpha$; $r = 0.997$). Phlogopites and biotites are not found in distinct fields, confirming the poor relationship between α and the octahedral chemical composition.

ACKNOWLEDGMENTS

REFERENCES CITED

Albee, A.L., and Ray, L. (1970) Correction factors for electron microanalysis of silicates, oxides, carbonates, phosphates and sulphates. Analytical Chemistry, 42, 1408–1414.

Bailey, S.W. (1984) Crystal chemistry of the true micas. In Mineralogical Society of America Reviews in Mineralogy, 13, 13–60.

Bell, I.A., and Wilson, C.J.L. (1977) Growth defects in metamorphic biotite. Physics and Chemistry of Minerals, 2, 153–169.

——— (1981) Deformation of biotite and muscovite: TEM microstructure and deformation model. Tectonophysics, 78, 201–228.

Bergerhoff, G., Kilger, B., Witthauer, C., Hundt, G., and Sievers, R. (1986) Inorganic crystal structure database. Institut für Anorganische Chemie der Universität, Bonn.

Bohlen, S.R., Peacor, D.R., and Essene, E.J. (1980) Crystal chemistry of a metamorphic biotite and its significance in water barometry. American Mineralogist, 65, 55–62.

Busing, W.R., Martin, K.O., and Levy, H.S. (1962) ORFLS, a Fortran crystallographic least-square program. U.S. National Technical Information Service, ORNL-TM-305.

Davoli, P. (1987) A crystal-chemical study of aegirin-augites and some evaluations of the oxidation state of Mn. Neues Jahrbuch für Mineralogie Abhandlungen, 158, 67–87.

——— (1989) Reciprocal lattice scan modes in single crystal diffractometry: A reexamination for cases of mineralogical interest. Zeitschrift für Kristallographie, 188, 11–29.

Donnay, G., Donnay, J.D.H., and Takeda, H. (1964) Trioctahedral one-layer micas. II. Prediction of the structure from composition and cell dimensions. Acta Crystallographica, 17, 1374–1381.

Einstein, J.R. (1974) Analysis of intensity measurements of Bragg reflections with a single crystal equatorial plane diffractometer. Journal of Applied Crystallography, 7, 331–344.

Ghose, S., Kersten, M., Langer, K., Rossi, G., and Ungaretti, L. (1986) Crystal field spectra and Jahn Teller effect of Mn^{3+} in clinopyroxene and clinoamphiboles from India. Physics and Chemistry of the Minerals, 13, 291–305.

Gregorkiewitz, M., and Rausell-Colom, J.A. (1987) Characterization and properties of a new synthetic silicate with highly charged mica-type layers. American Mineralogist, 72, 515–527.

Hamilton, W.C. (1965) Significance tests on the crystallographic R factor. Acta Crystallographica, 18, 502–510.

Hazen, R.M., and Burnham, C.W. (1973) The crystal structure of one-layer phlogopite and annite. American Mineralogist, 58, 889–990.

Hazen, R.M., Finger, L.W., and Velde, D. (1981) Crystal structures of a silica and alkali-rich trioctahedral mica. American Mineralogist, 66, 586–591.

Joswig, W. (1972) Neutronenbeugungsmessungen an einem 1M-phlogopit. Neues Jahrbuch für Mineralogie Monatshefte, 1–11.

Lin, J.C., and Guggenheim, S. (1983) The crystal structure of a Li, Be-rich brittle mica: A dioctahedral-trioctahedral intermediate. American Mineralogist, 68, 130–142.

Lipson, H., and Cochran, W. (1953) The crystalline state. Vol III. The determination of crystal structures. Bell and Sons, London.

McCauley, J.W., Newnham, R.E., and Gibbs, G.V. (1973) Crystal structure analysis of synthetic fluorphlogopite. American Mineralogist, 58, 249–254.

Meyrowitz, R. (1963) A semimicroprocedure for the determination of ferrous iron in nonrefractory silicate minerals. American Mineralogist, 48, 340–347.

Newnham, R.E., and Brindley, G.W. (1956) The crystal structure of dickite. Acta Crystallographica, 9, 759–764.

North, A.C.T., Phillips, D.C., and Mathews, F.S. (1968) A semi-empirical method of absorption correction. Acta Crystallographica, A24, 351–359.

Ohta, T., Takeda, H., and Takéuchi, Y. (1982) Mica polytypism: Similarities in the crystal structures of coexisting 1M and 2M₁ oxybiotite. American Mineralogist, 67, 298–310.

Pauling, L. (1930) The structure of micas and related minerals. Proceedings of the National Academy of Sciences, 16, 123–129.

Robinson, K., Gibbs, G.V., and Ribbe, P.H. (1971) Quadratic elongation, a quantitative measure of distortion in coordination polyhedra. Science, 172, 567–570.

Rossi, G. (1987) A review of the crystal-chemistry of clinopyroxenes in eclogites and other high pressure rocks. In Developments in petrology. Eclogites and eclogite facies rocks. Chapter 3. Elsevier Science Publishers, Amsterdam.

Rossi, G., Smith, D.C., Ungaretti, L., and Domeneghetti, M.C. (1983) Crystal chemistry and cation ordering in the system diopside-jadeite: A detailed study by crystal structure refinement. Contributions to Mineralogy and Petrology, 83, 247–258.

Rule, A.C., Bailey, S.W., Livi, K.J.T., and Veblen, D.R. (1987) Complex staking sequences in a lepidolite from Tørdal, Norway. American Mineralogist, 72, 1163–1169.

Smith, J.W., and Yoder, H.S. (1956) Experimental and theoretical studies of the mica polymorphs. Mineralogical Magazine, 31, 209–235.

Stout, G.H., and Jensen, L.H. (1968) X-ray structure determination: A practical guide. Macmillan Publishing, New York.

Takeda, H., and Ross, M. (1975) Mica polytypism: Dissimilarities in the crystal structures of coexisting 1M and 2M₁ biotite. American Mineralogist, 60, 1030–1040.

Takeda, H., and Morosin, B. (1975) Comparison of observed and predicted structural parameters of mica at high temperature. Acta Crystallographica, B31, 2444–2452.

Tokonami, M. (1965) Atomic scattering factor for O²⁻. Acta Crystallographica, 19, 486.

Toraya, H. (1981) Distortions of octahedra and octahedral sheets in 1M micas and the relation to their stability. Zeitschrift für Kristallographie, 157, 173–190.

Ungaretti, L. (1980) Recent developments in X-ray single crystal diffractometry applied to the crystal chemical study of amphiboles. Godisnjac Iugoslavenskog Centraza Kristalograiju, 15, 29–65.

Ungaretti, L., Lombardo, B., Domeneghetti, M.C., and Rossi, G. (1983) Crystal-chemical evolution of amphiboles from eclogitised rocks of the Sesia-Lanzo Zone, Italian Western Alps. Bulletin de Minéralogie, 106, 645–672.

Vainshtein, B.K. (1981) Modern crystallography. I. Symmetry of crystals, methods of structural crystallography. Springer-Verlag, Berlin.

Weiss, Z., Rieder, M., Chmielová, M., and Krajicek, J. (1985) Geometry of the octahedral coordination in micas: A review of refined structures. American Mineralogist, 70, 747–757.

Ziebold, T.O., and Ogilvie, R.E. (1964) An empirical method for electron microanalysis. Analytical Chemistry, 36, 322–327.